Rationalizing and functionalizing stannaspherene: Very stable stannaspherene "alloys"

ARTICLE *in* THE JOURNAL OF CHEMICAL PHYSICS · DECEMBER 2009

Impact Factor: 2.95 · DOI: 10.1063/1.3267046 · Source: PubMed

1 AUTHOR:

Aristides Zdetsis
University of Patras
125 PUBLICATIONS **1,584** CITATIONS

SEE PROFILE

Rationalizing and functionalizing stannaspherene: Very stable stannaspherene "alloys"

Aristides D. Zdetsis[a)]
Department of Physics, University of Patras, GR-26500 Patras, Greece

(Received 16 September 2009; accepted 3 November 2009; published online 10 December 2009)

It is illustrated here by *ab initio* calculations based on density functional theory and other high level methods that the high stability of the icosahedral Sn_{12}^{2-} dianion known as stannaspherene, reflects stability toward ionization rather than cohesion. This could be also connected with novel fluxional rearrangements and paths of Sn_{12}^{1-} leading eventually to Sn_{12}^{2-} involving charge transfer. In view of the very similar structural and electronic properties with the corresponding isovalent borane $(B_{12}H_{12})^{2-}$, it is demonstrated that stannaspherene can be further rationalized and functionalized on the basis of an isolobal analogy between group 14 clusters and isovalent boranes, carboranes, and bisboranes. Such analogy is of the same nature with analogous isolobal and isovalent similarities between silicon, hydrogenated silicon-carbon clusters and deltahedral boranes and carboranes, which the present author, scoptically and synoptically, has described as the "boron connection." It is predicted and verified theoretically: First, that the isovalent Bi_2Sn_{10} and Sb_2Sn_{10} clusters, considered as the microscopic analogs of tin-bismuth alloys, are very stable (more stable than stannaspherene itself) very symmetric and isolobal to Sn_{12}^{2-}; and second, that embedded clusters of the form $M@Sn_{12}^{2-}$, $M@Bi_2Sn_{10}$, M=Pt,Pd are very stable and highly symmetrical (I_h and D_{5d} respectively) with large highest occupied-lowest unoccupied molecular orbital gaps and very large embedding energies of the order of 5–6 eV. It is furthermore predicted that $Pt@Sn_{12}^{2-}$ and $Pt@Bi_2Sn_{10}$ can be synthesized in view of their higher stability compared to $Pt@Pb_{12}^{2-}$ which has already been synthesized. The marginal energy difference of 0.03 eV between the meta- and the para-isomer of Bi_2Sn_{10} indicates a fluxional behavior with respect to Bi–Sn interchange which should be related with the Sn_{12}^{1-} fluxionality leading eventually to Sn_{12}^{2-}. This rearrangement is also associated with a strange aromatic behavior. The same type of Bi–Sn fluxionality is also encountered in higher energy structures. Due to the "inert pair effect" in tin, the validity of the isolobal analogy is much stronger and fully valid compared to isovalent species based on germanium or silicon, such as Ge_{12}^{2-}, Bi_2Ge_{10}, and $Ge_{10}C_2H_2$ and Si_{12}^{2-}, Bi_2Si_{10}, and $Si_{10}C_2H_2$. The present ideas are in full agreement with available experiments and suggest even further functionalization of stannaspherene, analogous to metaloboranes, metalocarboranes, and stannaboranes with several potential applications. © *2009 American Institute of Physics*.
[doi:10.1063/1.3267046]

I. INTRODUCTION

Although carbon and silicon are the most important (for life and/or technology) elements of the 14th column of the periodical table, germanium, tin, and in part lead, become increasingly important in recent years for science and technology. In addition to carbon, silicon and mixed carbon-silicon nanostructures, nanosystems, and cluster composed structures, germanium, tin, and (less so) lead, can form many functional and important nanostructures which can be further functionalized.[1–10] Such functionalization can be usually accomplished through the methods and techniques of organometallic Chemistry for these materials directly or indirectly through isoelectronic and other analogies (such as the isolobal analogy)[11] to well known and well studied "similar materials."[6]

It is known for more than 30 years that chemical analogies, such as the *isolobal* analogy introduced through the pioneering work of Hoffman,[11] allow the correlation of seemingly very different chemical species, such as organic hydrocarbon fragments with transition metal ligands. The idea is very simple; the backbone of most organic compounds (hydrocarbons) is made up of the familiar groups CH_3, CH_2, and CH, and C, which can be put together at will. Thus, as Hoffman explains in his Nobel lecture,[11] any hydrocarbon may be constructed on paper from methyl groups, methylenes, methynes, and carbon atoms by substitution and introduction of heteroatoms. This way all of the skeletons and functional groupings imaginable, from ethane to tetrodotoxin, may be obtained. Two fragments are isolobal if the number, symmetry properties, approximate energy, and shape of the frontier orbitals and the number of electrons in them are similar (not identical[11]). CH, $Co(CO)_3$ and CH_3, $Mn(CO)_5$ can be considered as classical examples of isolobal fragments. As we can see from these examples, the isolobal pairs need not be isoelectronic. The isolobal analogy pro-

a)Electronic mail: zdetsis@upatras.gr.

vides a mechanism to predict new, hopefully stable, molecules, and compare molecular fragments with each other and with familiar species from organic Chemistry, offering also clues about reactivity and reaction mechanisms.

In this spirit, but not necessarily with the same reasoning, the present author, from the myriads of possible isolobal pairs, has attempted to "map" the structural chemistry of boranes and carboranes[12–17] to the structural chemistry of silicon and silicon-carbon clusters, respectively.[18–20] Boranes and carboranes constitute a very rich and well established branch of chemistry[12–17] with well known structural and stability rules[12–15] and powerful concepts.[16,17] Such well tested rules are generally lacking in the field of silicon and silicon carbon clusters, although electron-counting rules based on Wade–Mingos principles[13,15] have been used for silicon (and other) clusters, and some building-up rules have been suggested for silicon-carbon clusters[4] almost 15 years ago. This type of mapping was recently generalized[20(b)] to encompass many stable boron bearing compounds (e.g., boranes, carboranes, bisboranes, etc.), and extended to larger (than seven atoms) systems, and additional group 14 elements besides silicon, such as germanium and possibly tin. This extended and generalized analogy, which is only a very small, targeted, and rather unusual subset of the many existing or possible isolobal (and isoelectronic or isovalent) groups, with explicit reference to well known and well studied boranes, carboranes, and metalaboranes, has been scoptically and synoptically called by the present author "the boron connection." Independently of its name or the sense of humor of the author, the analogy of silicon (or other group 14) clusters with deltahedral boranes has been illustrated[6,18–20] to be very fruitful (independent of its full or partial success) in understanding, rationalizing, and functionalizing silicon and silicon-based clusters. It should be also mentioned that Zubarev *et al.*[21] have examined experimentally and theoretically small silicon cluster dianions such as Si_5^{2-} and Si_6^{2-} and have compared their structures with the corresponding boranes $(BH)_5^{2-}$ and $(BH)_6^{2-}$.

The boron connection and more generally the concept of isolobal analogy, is very simple and, as such, quite crude because the radial extent, the overlap and stabilization of the bonding levels could be different among isolobal fragments. Thus, there will be instances where it will fail with one (at least) of the fragments being unstable or dissimilar. Even in such instances this concept could be still useful although in a limited way.[18–20]

The idea of connecting the structural Chemistry of B_nH_n and Si_n clusters is not totally new but it goes back to Mingos and co-workers[22] and Wales[23] (in a rather different context). Also, Jemmis *et al.* have proposed an isolobal analogy between divalent silicon and trivalent boron,[24] while King *et al.*[16(b)] have considered the aromatic properties of Si clusters and boranes in parallel. Likewise, numerous authors have been freely using the Mingos-Wade electron-counting rules to rationalize electronic properties of silicon (and other) clusters (see for instance Refs. 6–8). Finally, beyond Si, for the isovalent Sn, Gädt and Wesemann[25] have extensively studied stanna-closo-dodecaborate chemistry, considering among others the $[SnB_{11}H_{11}]^{2-}$ dianion, homologous to $[1\text{-}CB_{11}H_{12}]^{1-}$ monocarbaborate anion, both related to $(B_{12}H_{12})^{2-}$ borane. This is formally equivalent to the idea of partially replacing one (BH) unit by Sn. In this respect the step of replacing formally all (not just one) BH units by Sn is easy to guess in the framework of the boron connection. As has been shown recently by the present author,[20(b)] due to the "inert pair effect,"[26–29] as we move down the period the structural and electronic similarity to boranes and carboranes gets better, although the energetical ordering between structures sometimes gets worse. This is particularly true for $n=12$, which is a very characteristic case because, although $B_{12}H_{12}^{2-}$ has a beautiful high symmetry icosahedral structure, the lowest energy isovalent silicon dianion is only C_s symmetric.[18(b),30] This is related with the better optimization of the sp^3 bonding and the uneven charge distribution in the C_s structure which facilitates the minimization of electrostatic repulsion.[27] Thus, in contrast to the $n=3-8$ case, for $n=12$ the full isolobal analogy

$$Si_n^{2-} \leftrightarrow Si_{n-2}C_2H_2 \Leftrightarrow (B_nH_n)^{2-} \leftrightarrow C_2B_{n-2}H_n, \tag{1}$$

is not valid for silicon structures if we are referring to the global minima.

Yet, even in this case: (a) the corresponding structures are low-lying local minima sharing several common properties, and (b) the trivial analogies $Si_n^{2-} \leftrightarrow Si_{n-2}C_2H$, and $(B_nH_n)^{2-} \leftrightarrow C_2B_{n-2}H_n$ hold separately true for the global minima providing however useful and fruitful information. In the same work[20(b)] it was also suggested that instead of two CH units in $Si_{n-2}C_2H_2$ we could use Bi or another group 15 element such as Sb with five valence electrons. In this case the generalized analogy would be

$$Bi_2Si_{n-2} \leftrightarrow Si_n^{2-} \leftrightarrow Si_{n-2}C_2H_2 \Leftrightarrow (B_nH_n)^{2-} \leftrightarrow C_2B_{n-2}H_n \leftrightarrow Bi_2B_{n-2}H_{n-2}, \tag{2}$$

which obviously for $n=12$ would be only partially valid (for silicon) as explained above.

For Ge_{12}^{2-} the energy difference of the C_s and I_h structures is only 0.03 eV at the CCSD(T)/TZVPP level of theory, in favor of the I_h structure, the "germanaspherene." This trend can be understood in terms of the *inert pair* effect,[26–29] or the larger *s-p* orbital energy separation which renders the sp^3 hybridization less instrumental[20(b)] for the bonding and binding of $(Ge_{12})^{2-}$, compared to $(Si_{12})^{2-}$. Following this trend one could anticipate that if we move further down to Sn, the energy difference between the C_s and I_h isomers would be further diminished or even reversed. This is indeed the case. The Sn_{12}^{2-} dianion is characterized by perfect I_h symmetry similar to $(B_{12}H_{12})^{2-}$, while the second lowest energy structure is indeed of C_s (near C_{2v}) symmetry similar to the one obtained for the Si_{12}^{2-} (and Ge_{12}^{2-}) dianion,[18(b)] separated by more than 0.77 eV from the second lowest. Thus the boron connection, which is based on the $BH^{2-} \rightarrow Si^{2-}$, $2BH^{1-} \rightarrow 2CH$ replacement rules,[18–20] is fully operative for Ge, Sn ($BH^{2-} \rightarrow Sn^{2-}$), and apparently for Pb (plumbaspherene) for which is much better valid. For Si_{12}^{2-} this analogy is only partially valid. Apparently this tendency could be related with the comment of Gädt and Wesemann[25] that the synthesis of the homologous $[SnB_{11}H_{11}]^{2-}$ was first

reported by Todd and co-workers since 1992 (Ref. 31) together with $[GeB_{11}H_{11}]^{2-}$ and $[PbB_{11}H_{11}]^{2-}$, but not of $[SiB_{11}H_{11}]^{2-}$. The full replacement of all BH units is a different matter. All this is in full agreement with the experimental and theoretical results of Cui *et al.*[32] and the recent synthesis of stannaspherene[32] and other tin clusters.[33]

Since for tin the boron connection is fully valid for n = 3–13, one can consider, as was explained earlier[20(b),37], alternative replacements of BH^{1-} units by other moieties with five valence electrons, such as bismuth or antimony as in Eq. (2)

$$Bi_2Sn_{n-2} \leftrightarrow Sn_n^{2-} \Leftrightarrow (B_nH_n)^{2-} \leftrightarrow Bi_2B_{n-2}H_{n-2}. \quad (3)$$

For n=12 in particular we would expect to have very stable $Sn_{10}Bi_2$ (or $Sn_{10}Sb_2$) clusters, since the corresponding bisboranes have been synthesized long time ago.[34] Our present calculations show that indeed this is the case: $Sn_{10}Bi_2$ with perfect D_{5d} symmetry is very stable (of comparable stability to stannaspherene itself) with large highest occupied molecular orbital (HOMO)-lowest unoccupied molecular orbital (LUMO) (H-L) gap.

The isolobal analogy (the boron connection) provides a unifying framework for such clusters which are considered as microscopic analogs of well known tin alloys, (useful in lithium-ion batteries and other composite materials[35,36]). In the case of $Si_{n-2}Bi_2$ clusters for n=7 for which the analogy (2) is fully valid, this idea has been successfully tested experimentally by Li *et al.*[37]

A. Computational Methods

The geometry optimizations (symmetry constrained and unconstrained) and single-point calculations for all structures were performed within the density functional theory (DFT), using the hybrid exchange and correlation functional of Becke-Lee, Parr, and Yang (B3LYP)[38] and the triple-valence-ζ doubly polarized (TZVPP) basis set.[39] This basis set, implemented in the TURBOMOLE program package[40] under the label def-TZVPP, is comparable to 6-311G(2df) quality. For Sn, Bi, and Sb, compatible effective core potentials (ECPs) were used which include scalar relativistic effects.[41] ECPs were also used for the embedding transition metals[41(a),42] (Pt, Pd, etc.). For comparison, in several critical cases involving small energy differences, the def2-TZVPP basis set[43] was used which includes the small-core ECPs.[44] No significant differences from the def-TZVPP results were found. To test the gas phase calculations of the dianions for solvation effects, the lowest energy structures of the dianions were recalculated by surrounding them by a sphere of 80 equal point charges of a total charge of +2e, to simulate a neutralized environment. In this case the HOMO and LUMO have clearly negative values and the H-L gaps of the low symmetry (second lowest energy) structures are reduced, although the H-L gaps of the high symmetry lowest energy structures remain practically unchanged. It must be emphasized that experimentally the relevant external charge distribution is rather asymmetric leading to structural distortions of the dianions, which are normally not reproduced by the gas phase calculations, even after the introduction of the spherical charge distributions as in the present calculations. In all cases numerous initial geometries were used [including the ones which are similar to those of Si_n^{2-} and $Si_{n-2}C_2H_2$, and in particular of Si_{12}^{2-} and $Si_{10}C_2H_2$, Refs. 18(b) and 20] which were generated in various possible ways including: (a) all (or most) conceivable substitutions (with or without scaling) on Si_n/Sn_n or $Si_n^{+/-(1,2)}/Sn_n^{+/-(1,2)}$ geometries (not only the lowest but all low-lying); (b) attachments in Si_{n-1}/Sn_{n-1} or $Si_{n-1}^{+/-(1,2)}/Sn_{n-1}^{+/-(1,2)}$ and Si_{n-2}/Sn_{n-2} or $Si_{n-2}^{+/-(1,2)}/Sn_{n-2}^{+/-(1,2)}$ geometries; and (c) best- and worst-case geometries generated by chemical intuition (based on valency and coordination) and symmetry. A plethora of structures was studied, leading to a practically exhaustive search. All these runs were performed without symmetry constrains using initially the TZVP basis set and the BP86 or B3LYP functional. The structures were afterwards reoptimized using the TZVPP basis set and the B3LYP functional, and symmetrized (using loose symmetry constrains initially) wherever possible. Frequency calculations were run for all structures. In cases of imaginary frequencies, new structures were generated by distorting the original structures according to the eigenvectors of the imaginary frequency modes and the process (optimization, vibration calculations) was repeated until the final structures have no imaginary frequencies. In all cases in which very small energy differences occurred, second order Møller-Plesset (MP2) perturbation theory was also used employing the same (def-TZVPP or simply TZVPP) basis set. Both DFT-B3LYP/TZVPP and MP2/TZVPP (single-point and geometry optimizations) calculations were performed with the TURBOMOLE program package.[36] In addition to MP2, in several critical cases single-point high level fourth order MP perturbation (MP4SDTQ), and coupled clusters theory CCSD(T) calculations were performed at both B3LYP/TZVPP and MP2/TZVPP geometries, using the same (def-TZVPP or TZVPP) basis sets and ECPs.[41,44] These calculations were performed with the GAUSSIAN program package,[45] which was also used for the nucleus-independent chemical shifts (NICS)[17] calculations employing the gauge-independent atomic orbital method (GIAO).

II. RESULTS

A. Comparison of Sn_n^{2-} (and Ge_n^{2-}) n=10–13, dianions

In Table I we have compiled the results of the calculations for Sn_n^{2-} and Ge_n^{2}, n=10, 11, 12, and 13. A large number of candidate structures was examined [some of which have been described in Ref. 18(b)], as described in the computational methods section. In Table I and Fig. 1 only the results for the lowest and second lowest structures are presented. The higher energy (up to about 2 eV) structures are shown in Fig. 2. All these structures correspond to singlet states. The corresponding triplet states are located higher in energy. For instance for n=10 the D_{4d} triplet is located 1.92 eV higher, however the Jahn–Teller distorted C_2 triplet is 1.24 eV higher than the D_{4d} lowest energy structure of the Sn_{10}^{2-} dianion. The smaller singlet-triplet separation is about 0.62 eV for the n=11, 13 C_{2v} lowest energy dianions. Thus it is obvious that some triplet states of low-lying structures

TABLE I. Comparison of the Sn_n^{2-} and Ge_n^{2-}, n=10–13, dianions at the B3LYP/TZVPP level of theory. The results include total energies E_{tot} (in hy), binding energies E_b and normalized binding energies E_b/n (in eV/atom), energy differences ΔE_{21}^{2-} between lowest and second lowest energy structures, H-L gaps, and energy differences between dianions and single anions, $\Delta E(-2,-1)$. These energies are in eV. NICS(0) values in ppm (parts per million) are also included. Results in parenthesis (in italics) correspond to the optimized MP2/TZVPP level. Numbers in brackets have been obtained by single-point MP4SDTQ (values in italics) and/or CCSD(T)/TZVPP calculations.

		n, Sym1			
Sn/Ge		$10D_{4d}$	$11C_{2v}$	$12I_h$	$13C_{2v}$
E_{tot}	Sn	−34.190 18(*−34.026 19*)	−37.5824(*−37.3970*)	−41.0168, −2572.1101[a](*−40.8055*) [−40.8674]	−44.4032(*−44.2377*) [−44.2549]
	Ge	−20 769.4933(*−20 756.0415*)	−22 846.4175	−24 923.3923	−27 000.2943
$E_b/(E_b/n)$	Sn	23.14(2.31)	24.96(2.27)	27.92,29.45[a](2.32)	29.59(2.28)
		28.77	31.11	34.83	36.57
	Ge	(2.88)	(2.83)	(2.90)	(2.81)
ΔE_{21}^{2-}	Sn	0.68(*0.65*)	0.44(*0.26*)	0.77(*0.39*)	0.20(*0.35*)
		0.87(*0.80*)	−0.26	0.36(*−0.39*) [0.03]	0.45
	Ge				
H-L	Sn	2.39	1.90	2.72,2.79[a]	1.98
		2.93	2.21	3.09	2.00
	Ge				
$\Delta E(-2, -1)$	Sn	0.22(*0.18*)	0.46(*0.26*)	−0.044, −0.029[a] (*0.313*),[*−0.36*][b],[−0.16]	0.41
	Ge	0.88	0.72	0.22	0.29
NICS(0)	Sn	−36.0	−8.1	+2.2	−46.0
	Ge	−51.1	−10.1	+9.6	−56.8

[a]Results obtained with the def2-TZVPP basis set (Ref. 43) using the small-core ECPs (Ref. 44).
[b]MP4(SDTQ) result with def-TZVPP basis set.

would be lower in energy than higher energy singlet states in Fig. 2. This is however, irrelevant for the purpose of the present paper. Table I includes for each Sn_n^{2-} and Ge_n^{2-} dianion the binding energy (E_b), the normalized binding energy E_b/n, the energy difference between second lowest and lowest energy structures (ΔE_{21}^{2-}), the H-L gaps, the energy difference between dianion and anion [$\Delta E(-2,-1)$], and the NICS(0) values. These results have been obtained with the DFT using the B3LYP functional and the quite large triple-valence-ζ double polarization basis set (TZVPP).

The binding energy of the dianions (in order to be electron precise) is defined relative to n−2 neutral Sn (and similarly Ge) atoms and two Sn^{1-} anions

$$E_b(Sn_n^{2-}/Ge_n^{2-}) = [(n-2)E(Sn/Ge) + 2E(Sn^{1-}/Ge^{1-})] - E(Sn_n^{2-}/Ge_n^{2-}), \quad (4)$$

where E(Sn/Ge) is the energy of Sn or Ge atom, $E(Sn^{1-}/Ge^{1-})$ is the energy of the corresponding anion, and $E(Sn_n^{2-}/Ge_n^{2-})$ is the energy of the dianion (not including the zero point energy).

As we can see in Fig. 1 (and Table I), the structural and energetic (energetic ordering) characteristics of these dian-

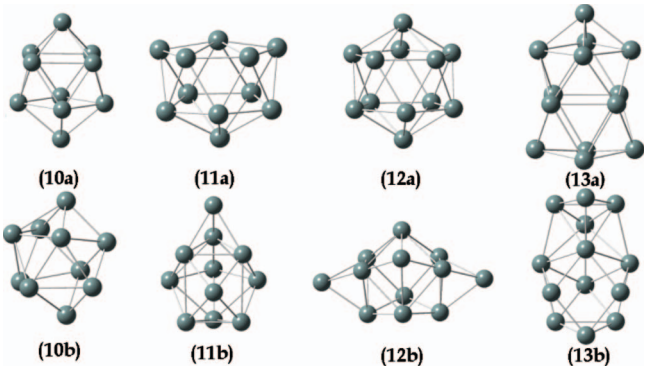

FIG. 1. The structures of the lowest (a) and second lowest (b) Sn_n^{2-}, n =10–13, dianions.

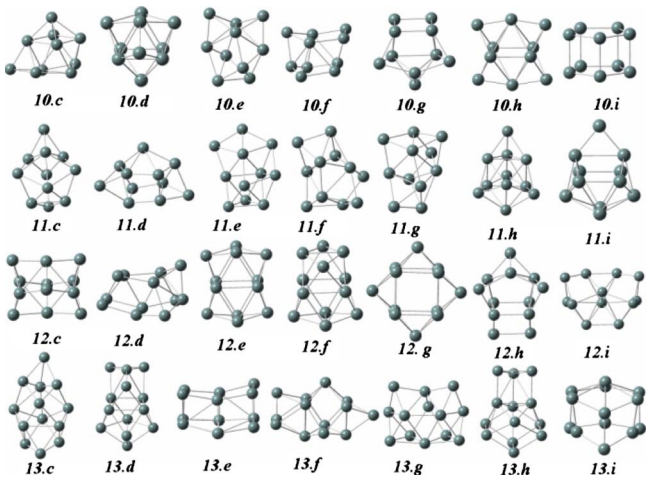

FIG. 2. The structures of the higher energy structures of Sn_n^{2-}, n=10–13, dianions, in the order of increasing energy.

ions are fully (and not partly, as in Si_n^{2-} and Ge_n^{2-})[18,20(b)] similar to the corresponding boranes $(B_nH_n)^{2-}$ as would be expected from the isolobal analogy-boron connection and the inert pair effect. This is also true for the electronic and aromatic characteristics.

For silicon[18,20(b)] and germanium[20(b)] only up to n=8 (and for n=10) the structures of the dianions are fully analogous to $(B_nH_n)^{2-}$. For this range of n, the structures of Si_n^{2-}, Ge_n^{2-}, and Sn_n^{2-} dianions are similar to each other and to the corresponding isovalent boranes.[18,20(b)] For n=9, 11, 12, and 13, the optimization of the sp^3 bonding dominates and establishes the geometry leading to low symmetry (C_s) structures[18,20(b)] for Si_n^{2-} and Ge_n^{2-}, which is a borderline case, in particular for n=12 where the I_h and C_s structures are very close to each other at the CCSD(T)/TZVPP level of theory. As was already explained, even for this case (n=12) the Si_{12}^{2-}, Bi_2Si_{10}, $Si_{10}C_2H_2$ structures are homologous and isolobal to each other, but, contrary to the corresponding tin based structures, not to the analogous boranes, bisboranes and carboranes. In the case of tin, for reasons already explained, these structures are fully determined by the powerful structural rules and stability laws[2–17] which determine the structures of the corresponding isovalent and isolobal boranes (and carboranes), shown in the first row of Fig. 1; whereas The C_s (near C_{2v} sometimes) structures are usually the second lowest energy structures, shown in the bottom row Fig. 1: (10b), (11b), (12b), and (13b). The n=12 is a special case. For Si_{12}^{2-} the C_s isomer is by far the lowest energy structure. For Ge_{12}^{2-} the B3LYP/TZVPP calculation predicts that the I_h isomer is the ground state by 0.36 eV lower than the C_s isomer. At the fourth order MP perturbation theory including single, double, triplet, and quadruplet excitations (MP4SDTQ) the difference is reduced to only 0.03 eV in favor of the I_h isomer. This is highly suggestive of fluxional behavior.[18] For Sn_{12}^{2-} the I_h symmetric isomer is clearly the ground state at all levels of theory. At the B3LYP/TZVPP level the energy difference of the I_h isomer from the second lowest energy C_s near C_{2v} isomer is 0.77 eV in excellent agreement with the value of 17.8 kcal/mol (0.772 eV) obtained by Cui *et al.*[32] (see supporting information in Ref. 32). The bond lengths of Sn_{12}^{2-} at the B3LYP/TZVPP level are 3.17 Å, but 3.13 Å at the MP2/TZVPP level of theory (the bond lengths quoted in Ref. 16 are 3.126 Å).

The normalized binding energies, E_b/n (per atom) for Sn_{12}^{2-} is almost equal to the one for Sn_{10}^{2-}, and is certainly lower than the corresponding atomization energies for Ge_n^{2-} dianions. Therefore it appears that this is not the best criterion for understanding the stability of stannaspherene. This is also true for the energy difference between the second lowest and the lowest energy structures, ΔE_{21}^{2-}, as well as the H-L energy gap which is a zeroth order approximation of the *chemical hardness*[26] of these clusters. Although Sn_{12}^{2-} is characterized by larger H-L gap compared to its "neighbors" (n=13, 11, and 10) it has smaller gaps than germanaspherene and other (n=10) germanium dianions. Neither the aromaticity index NICS(0) provides a satisfactory scale of stability in this case in view of the slightly antiaromatic +2.2 ppm value for Sn_{12}^{2-} and the more aromatic NICS(0) values of the other dianions. This will be discussed further below.

Thus, we need to examine a different criterion in the fourth column of Table I, based on the energy difference $\Delta E(-2,-1)$ between dianion and anion, since the most common way for a dianion to decay is by loosing one of the extra electrons, turning into a single anion. As we can see in Table I, among all dianions considered here only Sn_{12}^{2-} has lower total energy than the corresponding Sn_{12}^{1-} single anion at all levels of theory except MP2. The Sn_{12}^{1-} anion is characterized by C_{5v} symmetry, slightly distorted from the ideal I_h symmetry of Sn_{12}^{2-}, in agreement with the results of Cui *et al.*[32] The I_h symmetrical structure is also a local minimum of the anion, located 1 eV higher in energy (at the B3LYP/TZVPP level). Halfway between the I_h and C_{5v} anion (about 0.5 eV above the lowest energy C_{5v} structure) there is a D_{5d} symmetric structure which is a transition state with an imaginary frequency a_{2u} mode, which leads after distortion and optimization to the C_{5v} global minimum of the anion. As we can see in Table I, the B3LYP method predicts a small negative total energy difference between anion and dianion of −0.044 eV, whereas the MP4SDTQ calculation reveals a much larger difference of −0.36 eV, which at the CCSD(T) level finalizes to the value of −0.16 eV. This value is in excellent agreement with the value of −0.157 eV deduced from the total energy values of Cui *et al.*[32] (in their supporting information), obtained by using the two-component relativistic DFT method with the zero-order regular approximation, the PW91 functional, and the ADF/TZVPP basis set. Thus for Sn_{12}^{2-} the total energy of the dianion is lower than the total energy of the anion. This is a unique property which could explain the high stability of stannaspherene. From the electronic configuration(s) (and the other data which will be discussed later) of Table II, this can be understood in terms of the closure of the highly (fivefold) degenerate h_g HOMO orbital of Sn_{12}^{2-}. The same argument does not apply to Si_{12}^{2-} and (in part) Ge_{12}^{2-} for which the icosahedral structure is not the lowest energy structure of the dianion.

It should be clear that, despite the fact that the dianion has slightly lower total energy compared to the single anion, the binding energy of the single anion, defined similarly to Eq, (4) by

$$E_b(Sn_n^{1-}/Ge_n^{1-}) = [(n-1)E(Sn/Ge) + E(Sn^{1-}/Ge^{1-})] - E(Sn_n^{1-}/Ge_n^{1-}), \quad (5)$$

in obvious notation, is higher than the dianion binding energy. For stannaspherene (n=12) we find $E_b(Sn_{12}^{1-})=29.06$ eV in comparison to $E_b(Sn_{12}^{2-})=27.92$ eV for the dianion, a difference of 1.14 eV at the B3LYP/def-TZVPP level of theory. At the B3LYP/def2-TZVPP level we obtain $E_b(Sn_{12}^{1-})=30.57$ eV and $E_b(Sn_{12}^{2-})=29.45$ eV respectively (a difference of 1.12 eV).

The calculated adiabatic detachment energy at the B3LYP/TZVPP level is 3.05 eV and the vertical detachment energy is 3.18 eV. These values, although slightly underestimated are in generally good agreement with the measured values of 3.23 and 3.34 eV, respectively.[32]

The MP2 (geometry optimization and total energy) method, on the contrary, gives very different results, favoring the single ion by +0.31 eV. Therefore MP2 should not be

TABLE II. Total (E) and relative (ΔE) energies, electronic configurations (e-configur.), and harmonic frequencies (and symmetries) of Sn_{12}^{2-}, and various candidate structures (Struct.) of Sn_{12}^{1-} characterized by their symmetry (Sym.) The frequencies of high intensity modes (more than 40% of the peak intensity) are given in bold numbers, whereas those with intensity higher than 90% are also underlined.

Struct.	Sym.	E (hy)/ΔE (eV)	E-configur.	Frequencies (cm^{-1})/(symmetries)
Sn_{12}^{2-}	I_h	**−41.0168**	$1t_{2u}^6 2a_g^2 1g_u^8$	62.8(h_u), 70.5(h_g), 91.6(g_g), 103.0(t_{2u}), 105.8(g_u), 114.6(h_g),
		0	$2t_{1u}^6 2h_g^{10}$	118.6(a_g), **<u>121.8</u>**(t_{1u}),
Sn_{12}^{1-}	I_h	**−40.9935**	$1t_{2u}^6 2a_g^2 1g_u^8$	62.9(h_u), 71.2(h_g), 92.3(g_g), 105.2(t_{2u}), 106.1(g_u), 115.1(h_g),
		+0.63	$2t_{1u}^6 2h_g^9$	120.5(a_g), and **<u>123.4</u>**(t_{1u})
Sn_{12}^{1-}	C_i	**−41.0127**	…	Imaginary frequency $a_u(\rightarrow C_{5v})$
				56.9(a_u), 57.0(a_u), 57.2(a_u), 57.3(a_u), 66.1(a_u), 67.2(a_g),
			$8a_g^2 9a_g^2$	67.5(a_g), 72.7(a_g), 72.8(a_g), 73.0(a_g), 87.8(a_g), 88.0(a_g),
			$11a_u^2\ 12a_u^2$	93.8(a_g), 93.9(a_g), 102.9(a_u), 103.1(a_u), 105.1(a_u),
			$10a_g^2\ 11a_g^2$	105.2(a_u), 102.9(a_u), 107.0(a_g), 108.8(a_u), 108.9(a_u),
				115.0(a_g), 115.2(a_g), 119.3(a_g), **120.3**(a_u), 123.1(a_g),
		+0.11	$13a_u^2 12a_g^1$	123.3(a_u), **<u>124.9</u>**(**a_u**), and **<u>125.1</u>**(a_u)
Sn_{12}^{1-}	D_{5d}	**−41.0128**	…	Imaginary frequency $a_{2u}(\rightarrow C_{5v})$
			$2e_{2g}^4 3a_{2u}^2$	56.9(e_{2u}), 57.1(e_{1u}), 65.9(a_{1u}), 67.4(e_{2g}), 72.8(e_{1g}),
			$3e_{1u}^2 e_{1g}^4$	72.8(a_{1g}), 87.8(e_{1g}), 93.8(e_{2g}), 102.9(e_{2u}), 105.2(e_{2u}),
		+0.11	$4a_{1g}^2 3a_{2u}^1$	107.0(a_{1g}), 108.7(e_{1u}), 115.0(e_{1g}), 119.2(a_{1g}), **120.3**(a_{2u}),
				123.2(e_{2g}), and **<u>125.0</u>**(e_{1u})
Sn_{12}^{1-}	C_{5v}	**−41.0152**	…	54.8(e_1), 58.3(e_2), 66.8(a_2), 67.4(e_1), 68.9(e_2), 69.5(a_1),
			$5a_1^2 3e_1^4 3e_2^4$	86.4(e_2), 90.8(a_1), 91.4(e_1), 99.9(e_2), 102.8(a_1),
		+0.04	$4e_1^4 6a_1^2$	104.0(e_2), 109.1(e_1), **117.2**(a_1), **117.3**(e_1), 119.8(e_2),
			$4e_2^4 5e_1^4 7a_1^1$	**121.4**(a_1), and **<u>131.5</u>**(e_1)

reliable in this case. Earlier experience with magic silicon clusters, Si_6 in particular, has shown[18(a),42] that in such cases (of small energies differences related with possible fluxional behavior) the MP2 method should not be trusted due to poor convergence of the perturbation expansion.[18(a),46] For the other dianions in Table I (which are not fluxional) the MP2 and B3LYP [and CCSD(T) wherever available] results follow the same trends and relative magnitudes We should therefore interpret the results of Table I for Sn_{12}^{2-} on the basis of the B3LYP and CCSD(T) methods only. On the basis of such interpretation the exceptional stability of stannaspherene should be associated with stability against ionization toward single anion (and obviously toward neutral cluster), which could be also understood in terms of the closure of the HOMO $2h_g$ orbital holding 10 valence electrons in the dianion [and the hole in the high symmetry anion(s), as shown in Table II]. Moreover (in view of the rather small energy difference, the presence of a higher "suspiciously stable dynamically" local minimum of the anion with the same I_h symmetry and the intermediate D_{5d} symmetric transition state) it is tempting to conceive this as a special case of a fluxional path (behavior), which should proceed through the intermediate D_{5d} and the almost identical C_i structure(s), of the single anion ending up at the dianion (and back). It should be emphasized that both intermediate D_{5d} and C_i structures have been obtained by unconstrained (C_1) geometry optimization (and afterwards symmetrization) starting from different initial geometries. As we can see in Table II, the vibrational and energetic (total energies) characteristics of these structures, are practically identical. However, they are clearly distinct (but related) and could be considered as different instances of the same "multistructure" within the fluxional interpretation. The suggested fluxional behavior does not necessarily signify lower stability. On the contrary, according to an earlier conjecture of the present author,[18(a)] this type of fluxional behavior could be considered as a "signature of magicity," as in the case of Si_6 and in part Si_{10} magic clusters.[18(a),46] This behavior could be also conceived as a manifestation of dynamic Jahn–Teller effect as in the case of Si_6.[18(a),46,47] Yet, in this case the fluxional behavior of the single anion would be associated with charge transfer leading to the dianion. If this is the case we would have a totally different novel effect, which, however, could be characterized by the first order Jahn–Teller effect. This, however, is just a speculation at this time which needs further and deeper investigation.

B. Comparison of Si_{12}^{2-}, Ge_{12}^{2-}, Sn_{12}^{2-}, and Pb_{12}^{2-} dianions

In this section we will describe the vertical variation in atomization energy, H-L gap, and NICS(0) values for the n = 12 I_h—symmetric dianions as we go down the period. As we can see in Table III, although the variation in atomization energy shows a clear and systematic decrease (apparently related to the reduction of covalent bonding), the H-L

TABLE III. Variation in the atomization energy E_a, H-L gap, NICS(0), and h_g-t_{1u} occupied orbital energy separation, as we go down the period from Si_{12}^{2-} to Pb_{12}^{2-}.

	Si_{12}^{2-}	Ge_{12}^{2-}	Sn_{12}^{2-}	Pb_{12}^{2-}
E_a (eV)	3.28	3.02	2.52	2.40
H-L (eV)	2.68	3.09	2.72	3.08
NICS (0) (ppm)	+46.6	+9.6	+2.2	−8.4
h_g-t_{1u} (eV)	+0.83	+0.40	+0.16	−0.07

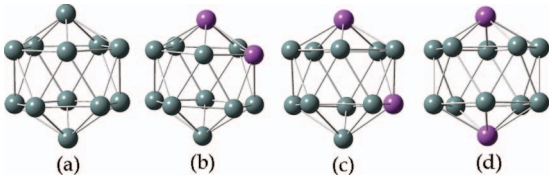

FIG. 3. The lowest energy structures (in reverse order) of $Sn_{10}Bi_2$, and $Sn_{10}Sb_2$ obtained from Sn_{12}^{2-} (a), by ortho- substitutions (b), meta- substitutions (c), and para- substitutions (d).

(Kohn–Sham) gap shows no clear trend. Yet the most interesting property in this case is the variation of the aromaticity index[17] NICS(0). As we have seen in the last row of Table I, the NICS(0) value for Sn_{12}^{2-} (and Ge_{12}^{2-}) is positive (paratropic), contrary to the rest of the dianions, and contrary to the corresponding NICS(0) value of the isovalent and isostructural and isolobal $(B_{12}H_{12})^{2-}$ borane.

As has been explained earlier,[16(b),18,20(b)] this is related to the high symmetry of the structure(s), as in the n=6 case,[18] and the resulting mixing of very paratropic five-fold degenerate h_g orbitals. These orbitals are the HOMO orbitals for the dianions of Table I, while the diatropic threefold degenerate t_{1u} orbitals are just bellow, HOMO-1 orbitals, (see the electron configuration of Sn_{12}^{2-} in Table II). In the corresponding $(B_{12}H_{12})^{2-}$ borane, which is characterized by a diatropic NICS(0) value of −28.9 ppm,[20(b)] the h_g is the HOMO-1 orbital, 0.46 eV below the HOMO. To better expose the influence of the h_g and t_{1u} orbitals in the aromatic properties we have tabulated the values of the h_g-t_{1u} orbital energy separation bellow the NICS(0) values. The correlation between the two is evident.

C. Bismuth and antimony stannaspherene "alloys"

On the basis of the earlier work[18(b),20(b),27] on Si_{12}^{2-}, Ge_{12}^{2-}, $Si_{10}C_2H_2$, and $Ge_{10}C_2H_2$, and the initial geometries considered there, as well as an additional large number of diverse structures generated by intuition and experience, we have optimized (without any constrain) a plethora of initial geometries for $Sn_{10}Bi_2$ (and $Sn_{10}Sb_2$), based (among many others) on icosahedral, octahedral, and hexagonal motifs. Among all these structures the lowest energy structures are, by far, those obtained by ortho-, meta-, and para-bismuth substitutions on the icosohedral Sn_{12}^{2-} dianion, shown in Figs. 3(b)–3(d).

The higher energy structures, up to 2 eV, are shown in the order of increasing energy in Fig. 4. Structures above 2 eV are not shown here. In view of the very large number of structures examined and the practically exhaustive search we have performed, the high (D_{5d}) symmetry para-isomer in Fig. 3(d) can be safely identified as the global minimum with a marginal energy difference (of 0.03 eV) from the meta-isomer in Fig. 3(c), and a difference of 0.27 eV from the third lowest ortho-isomer in Fig. 3(b).

The C_s almost C_{2v} structure obtained by "para-" substitution (with the bismuth atoms far apart) from the second lowest Sn_{12}^{2-} dianion of Fig. 1, (12b), is the fourth lowest energy structure located 0.79 eV higher from the global minimum para-isomer. This C_s/C_{2v} isomer is shown in (4) in

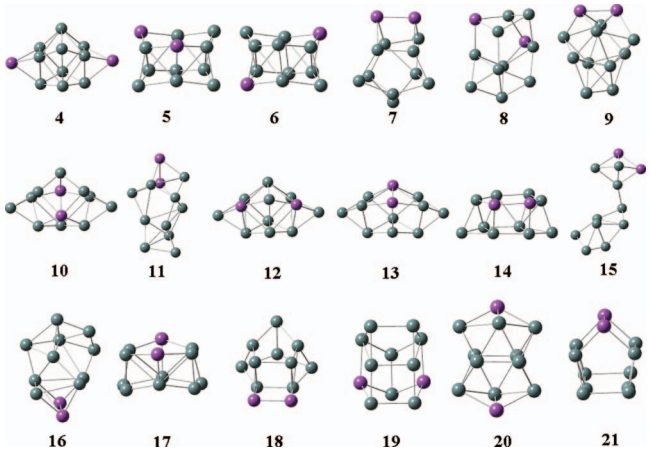

FIG. 4. The higher energy structures of $Sn_{10}Bi_2$ (and $Sn_{10}Sb_2$). The numbers below the structures indicate their energetical ordering.

Fig. 4 together with the rest structures which are located up to 2 eV above the three "icosahedral" isomers. The ortho-<meta-<para- stability ordering of the three lowest energy structures (in Fig. 3) is consistent with the ordering of the corresponding isovalent (and isolobal) carboranes, which in turn is consistent with empirical stability rules and criteria.[20(b)] Yet for the corresponding $Bi_2B_{10}H_{10}$ bisboranes, the 1, 2-orthoisomer is lowest in energy (this is also true for the isovalent and isolobal $Bi_2B_5H_5$, Bi_2Si_5 clusters[37]). This difference must be related, among others, with the relative strength of Bi–Bi and Bi–B (or Bi–Sn) bonds, and the size mismatch of the boron and bismuth (or Si, Bi) atoms. For $Sn_{10}Bi_2$ there is not such mismatch.

The main characteristics (cohesive, energetic, electronic, structural, and aromatic) of the four lowest energy isomers of $Sn_{10}Bi_2$ and $Sn_{10}Sb_2$ have been compiled in a concise form in Table IV. As we can see in this table, the para-, meta-, and ortho-isomers of $Sn_{10}Bi_2$ are of comparable stability (binding energy) with stannaspherene and the same isomers of $Sn_{10}Bi_2$ have much larger binding energies than stannaspherene itself. Yet the larger binding energy does not always mean and larger stability in view of other factors (kinetic effects) which can also influence the observed stability. The energetic ordering and the H-L gaps in the second and third rows of the table, scale well with the variation in binding energy. The final row of the table, lists of the NICS(0) values, which for the three lowest energy structures generated from the I_h Sn_{12}^{2-} dianion "fluctuate" around the weakly paratropic dianion value of 2.2 ppm. Yet, due to the lower symmetry and the presence of bismuth (or antimony), the NiCS(0) value of the D_{5d} symmetric para-isomer in Fig. 3(d) is now weakly diatropic (aromatic). As a matter of fact all NICS(0) values in Table V, except the $Sn_{10}Sb_2$ ortho-isomer are more aromatic (or less antiaromatic) compared to the corresponding +2.2 ppm value of stannaspherene. The higher energy lower symmetry C_s isomer has a large diatropic NICS(0) value similar to the corresponding value of the C_s second lower-energy dianion structure of 12(b) in Fig. 1. This value is of the same magnitude and sign with the diatropic values of the corresponding isovalent C_s dianions[18(b),20(b)] of Si_{12}^{2-} and Ge_{12}^{2-}.

TABLE IV. Binding energies (E_b), Energy differences (ΔE), H-L gaps (H-L), average distances (Bi–Bi, Bi–Sn, and Sn–Sn), together with NICS(0) values for the lowest energy $Sn_{10}Bi_2$ and $Sn_{10}Sb_2$ isomers. Reference energy in atomic units (hy) of the D_{5d} para-isomer: Def-B3LYP=−44.993598, Def-MP2=−44.724065, Def2-B3LYP=−2572.718803, and Def2-MP2=−2566.189192.

		D_{5d} para-	C_{2v} meta-	C_{2v} ortho-	C_s/C_{2v} (from C_s)
E_b (eV)	Bi	27.75,29.03[a]	27.72	27.45	26.96
	Sb	28.50	27.99	24.44	19.93
ΔE (eV)	Bi	0.0	0.029, 0.024[a] (0.051), (0.063)[a]	0.274,0.244[a]	0.786,0.963[a]
	Sb	0.0	0.042	0.338	0.714
H-L (eV)	Bi	2.48,2.52[a]	2.38, 2.41[a]	2.32,2.35[a]	1.54,2.00[a]
	Sb	2.53	2.42	2.33	1.97
(Å)	Bi–Bi, Sn–Bi, Sn–Sn	5.83,3.14,3.21	4.93, 3.15, 3.22	3.13,3.17,3.18	8.54,3.02,3.00
	Sb–Sb, Sn–Sb, Sn–Sn	5.69,3.08,3.21	4.81, 3.10, 3.22	2.98,3.11,3.18	8.34,2.88,3.02
NICS (ppm)	Bi	−2.21	+0.23	+1.99	−15.87
	Sb	−1.51	+1.70	+3.11	−15.24

[a]Results obtained with the def2-TZVPP basis set (Ref. 43) using the small-core ECPs (Ref. 44).

We can also notice in Table IV, that the aromaticity as expressed by values and sign of NICS(0), correlates well with the variation of the Bi–Bi (and Sb–Sb) distance (shown in the fourth row of Table IV): the larger the Bi–Bi (or Sb–Sb) distance, the larger the aromaticity. This seems to indicate that besides high symmetry, the overlapping Bi–Bi (or Sb–Sb) orbitals contribute significantly to antiaromaticity. We can verify, therefore that all properties of $Sn_{10}Bi_2$ (and $Sn_{10}Sb_2$) clusters are in direct relation to the corresponding properties of stannaspherene (and to the corresponding carboranes and bisboranes). This is also reflected in the structure of their HOMO and LUMO orbitals, shown in Fig. 5. As a final comment on the results of Table IV we can observe that, although the D_{5d} symmetric lowest energy $Sn_{10}Bi_2$ and $Sn_{10}Sb_2$ structures have weakly aromatic (rather than antiaromatic, as stannaspherene) NICS(0) values, they, nevertheless, are characterized by similar structural and electronic properties as stannaspherene. This can be further verified by examining the structure of the H-L orbitals of $Sn_{10}Bi_2$, in comparison to the same orbitals of Sn_{12}^{2-}, shown in Fig. 5. As we can see in Fig. 5, HOMO and LUMO, as well as charge densities are similar and homologous.

For the higher energy structures of Fig. 4 some energetic (relative energy ΔE), structural (symmetry, sym.) and electronic (H-L gaps) characteristics have been summarized in Table V. As we can see in Table V, similarly to the lowest energy structure(s), there are several other structures with marginal energy differences (of about 0.005–0.02 eV) which are similar but with different "substitutions" of Bi atoms (see for example, structures 5–6 and 12–13). These structures could be characterized as fluxional with respect to Bi–Sn interchange. This type of fluxionality could be apparently related to the Sn_{12}^{2-}–Sn_{12}^{1-} "fluxionality" discussed above in relation to the stability of stannaspherene. This could be a very interesting and novel effect demanding further investigation.

There are also other accidentally isonergetic structures, such as 4–5 and 13–14, which are characterized by a rather different structural framework. We can also observe that the energetical ordering of the structures 4, 10, 12, and 13, obtained from the C_s/C_{2v} second lowest structure of Sn_{12}^{2-} (in 12b in Fig. 1) is similar (relative Bi–Bi distance) to the

TABLE V. Structural and energetic characteristics of the "lowest" isomers of $Sn_{10}Bi_2$.

Struct.	Sym	H-L (eV)	ΔE (eV)
(1) 2.d	D_{5d}	2.48	0.00
(2) 2.b	C_{2v}	2.38	0.02
(3) 2.c	C_{2v}	2.32	0.27
(4) 3.4	C_{2v}/C_s	2.04	0.78(6)
(5) 3.5	C_s	2.18(3)	0.79(4)
(6) 3.6	C_{2h}	2.17(9)	0.79(5)
(7) 3.7	C_1	1.86	0.85
(8) 3.8	C_1	1.53	0.92
(9) 3.9	C_2	1.47	1.11
(10) 3.10	C_{2v}/C_s	1.77	1.16
(11) 3.11	C_1	1.83	1.18
(12) 3.12	C_{2v}/C_s	1.65	1.28(0)
(13) 3.13	C_{2v}/C_s	1.69	1.28(9)
(14) 3.14	C_1	1.91	1.29(1)
(15) 3.15	C_1	1.19	1.51
(16) 3.16	C_1	1.66	1.53
(17) 3.17	C_s	1.49	1.65
(18) 3.18	C_s	0.77	1.76
(19) 3.19	C_s	1.62	1.81(8)
(20) 3.20	C_{2h}	1.13	1.82(2)
(21) 3.21	C_{2v}	1.19	2.22

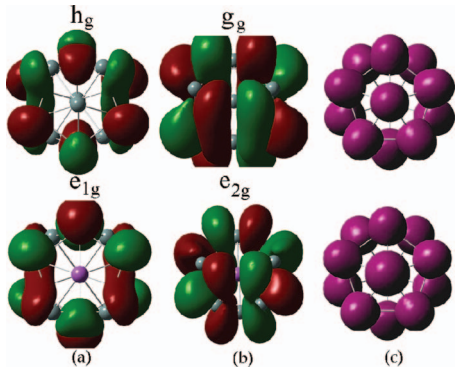

FIG. 5. Comparison of the electronic structure of Sn_{12}^{2-} (top) and $Sn_{10}Bi_2$ (bottom): (a) HOMO, (b) LUMO (both with isovalue of 0.02), and (c) total charge density (isovalue=0.2).

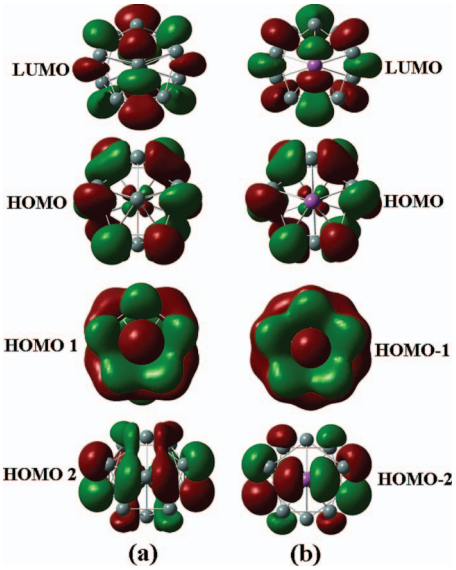

FIG. 6. The HOMO and LUMO orbitals of $Pt@Sn_{12}^{2-}$ left (a) of g_g and h_g symmetries respectively, in comparison to those of and $Pt@Sn_{10}Bi_2$ (b) on the right, with symmetries from top to bottom of e_{2g} (LUMO), e_{1g} (HOMO), a_{1g} (HOMO-1), and e_{2g} (HOMO-2) respectively.

para-> meta-> ortho-ordering of the lowest three icosahedral isomers. In general, there is an overall gross correlation of the energetical ordering and the H-L gap, as would be expected from the fact that the H-L gaps are a zero-order measure of the chemical hardness.

D. Further functionalization of Sn_{12}^{2-} and $Sn_{10}Bi_2$

Similarly to organometalic carboranes and $Si_{n-2}C_2H_2$ clusters,[20] stannaspherene and $Sn_{10}Bi_2$ (and $Sn_{10}Sb_2$) clusters can be further functionalized in several different ways following analogous functionalization of carboranes, bisboranes and stannaboranes. As a first example we can consider doping with transition metals. Gädt and Wesemann[25] in their study of stanna-closo-dodecaborate chemistry concluded among others that the high stability $[SnB_{11}H_{11}]^{2-}$ can be regarded as a special tin(II) ligand and its metal complexes can be compared to the plethora of transition metal coordination compounds with a large variety of tin(II) ligands. On the basis of the isolobal analogy it would be expected that the same would be true for Sn_{12}^{2-} (stannaspherene) and $Sn_{10}Bi_2$. Here we have considered as an example the $M@Sn_{12}^{2-}$ and $M@Sn_{10}Bi_2$, with M=Pt,Pd. As we can see in Fig. 6 and Table VI, these metal complexes are isovalent and isolobal to each other, very stable and highly symmetric (of I_h and D_{5d} symmetry respectively). The corresponding $Pt@Pb_{12}^{2-}$ complex for plumbaspherene has been already synthesized.[48] It is interesting to compare the stability of $Pt@Pb_{12}^{2-}$ with that of $Pt@Sn_{12}^{2-}$. On the basis of the *embedding* or *inclusion* energy, $Pt@Sn_{12}^{2-}$ is more stable than $Pt@Pb_{12}^{2-}$, and $Pt@Sn_{10}Bi_2$ is more stable than both of them. This is highly suggestive that $Pt@Sn_{10}Bi_2$ (and $Pt@Sn_{12}^{2-}$) could be synthesized as well. The embedding energy for $M@Sn_{12}^{2-}$, M=Pt,Pd, is defined as

TABLE VI. Embedding energies (E_{emb}), and H-L gaps (H-L) in eV, together with symmetries of the HOMO and LUMO orbitals of $M@Sn_{12}^{2-}$, $M@Sn_{10}Bi_2$, (M=Pt,Pd), and $Pt@Pb_{12}^{2-}$.

Structure	E_{emb} (eV)	H-L (eV)/sym
$Pt@Sn_{12}^{2-}$	5.76	2.43 (h_g-g_g)
$Pd@Sn_{12}^{2-}$	4.07	2.49 (h_g-g_g)
$Pt@Pb_{12}^{2-}$	5.27	2.79 (h_g-g_g)
$Pt@Bi_2Sn_{10}$	5.95	2.25(e_{1g}-e_{2g})
$Pd@Sn_{10}Bi_2$	4.22	2.29(e_{1g}-e_{2g})

$$E_{emb} = \{E[M] + E[Sn_{12}^{2-}]\} - E[M@Sn_{12}^{2-}] \quad (6)$$

and similarly for $M@Sn_{10}Bi_2$ and $Pt@Pb_{12}^{2-}$. In this definition $E[M@Sn_{12}^{2-}]$ is the total energy of the embedded cage, E[M] is the energy of the embedding transition metal atom, and $E[Sn_{12}^{2-}]$ is the cage energy (stannaspherene, or plumbaspherene dianions or neutral $Sn_{10}Bi_2$).

The stability of all these species is also reflected in the rather large H-L gaps (which are a zero-order measure of the chemical hardness) and is related to shell closure of the 10th-fold degenerated $3h_g$ molecular orbital in Sn_{12}^{2-} (and Pb_{12}^{2-}) and the fourth fold $3e_g$ degenerate orbital in $Sn_{10}Bi_2$.

We can also observe that the embedding energy (the energy gain) is smaller for Pd compared to Pt in all cases, but again $Pd@Sn_{10}Bi_2$ is more stable than $Pd@Sn_{12}^{2-}$. There is reasonable hope, therefore, that $Pt@Sn_{10}Bi_2$ and $Sn_{10}Bi_2$ could be synthesized (together with $Pt@Sn_{12}^{2-}$). Furthermore, on the basis of the isolobal analogy and the work of Gädt and Wesemann[25] it could be further anticipated or even predicted that ligands of the form $[CHSn_{11}]^{1-}$ or $[Au_2(Sn_{12})_2(PPh_3)_2]^{2-}$, or $[Au_2(Sn_{12})_3(PPh_3)_2]^{4-}$, etc., should be particularly stable. This remains to be seen.

As an additional example of possible functionalization for $Sn_{10}Bi_2$ one could consider also structures analogous to carborods, discussed by Yang *et al.*[49] Some simple such "analogous" structures are shown in Fig. 7.

All four structures shown in Fig. 7 are local minima (low

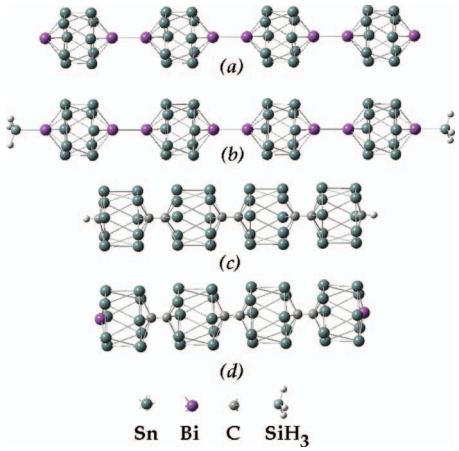

FIG. 7. Chains of $Sn_{10}Bi_2$ and $Sn_{10}C_2H_2$ in the form $[Sn_{10}Bi_2]_4$ (a), $[Sn_{10}Bi_2]_4[SiH_3]_2$ (b), $[Sn_{10}C_2H]_4$ (c), and $[Sn_{10}C_2]_2[Sn_{10}CBi]_2$ (d), based on "analogous" carborane structures by Yang *et al.* (Ref. 49).

lying energetically), which although of D_{5d} symmetry originally, they turn most of them (after optimization and distortion according to the imaginary frequency modes) into C_{2h} symmetrical structures.

III. CONCLUSIONS

It has been shown that by invoking the isolobal analogy, which for synoptical and scoptical reasons, was called the boron connection by the present author, we can further rationalize and functionalize stannaspherene and other group 14 dianions. It has been shown that this analogy is fully operative for Sn_{12}^{2-} (and all tin dianions n=6–13), Pt_{12}^{2-}, and Ge_{12}^{2-} as a borderline case; while is only partially valid for Si_{12}^{2-} with the broader meaning of the term. These differences are attributed to the increasing tendency toward divalent species as we move down the 14th column (in the present case) of the periodical table (inert pair effect).

On the basis of the boron connection it has been predicted that $Sn_{10}Bi_2$ and $Sn_{10}Sb_2$ clusters, which can be considered as the microscopic analogs of the well known tin-bismuth (and tin-antimony) alloys are very stable (of equal or greater stability than stannaspherene itself) highly symmetrical and isolobal to stannaspherene. These cages can be further functionalized.

It is also predicted on the basis of this isolobal analogy and known results from stanna-closo-dodecaborate chemistry;[25] that the Pt (and other transition metal atom) doped cages $Pt@Sn_{12}^{2-}$ and $Pt@Sn_{10}Bi_2$ would be very stable (with $Pt@Sn_{10}Bi_2$ more stable than $Pt@Sn_{12}^{2-}$) and as a matter of fact more stable than the corresponding isovalent $Pt@Pb_{12}^{2-}$ which has been already synthesized. This is highly suggestive that both $Pt@Sn_{12}^{2-}$ and $Pt@Sn_{10}Bi_2$ could be synthesized as well.

It has been illustrated that the aromatic properties of these clusters can be tuned from weakly antiaromatic (as in stannaspherene) to weakly aromatic, thus facilitating the design of complex materials responding in a reverse and/or direct way in an external magnetic field. These types of materials could be proven appropriate for the design of natural optically left-handed materials, assuming that such materials should be composed of subunits (rings) responded in an opposite way to the magnetic field (in analogy to aromatic and antiaromatic behavior) of the electromagnetic radiation. This is only an oversimplified speculation at the present time.

It has been also illustrated that the stability of stannaspherene is actually due to stability against ionization toward Sn_{12}^{1-} (and Sn_{12}) rather than to cohesive stability. On top of this it has been illustrated and suggested that between stannaspherene and the Sn_{12}^{1-} single ion there are possible fluxional rearrangement paths, which apparently involve charge transfer. This novel effect could be responsible for the ("dynamical") stability of stannaspherene in the light of earlier suggestion of the present author[18(a)] that this type of fluxionality is strongly connected to (or related with) magicity (high stability). This interpretation could also explain the very high stability of the "functionalized" $Sn_{10}Bi_2$ (alloy) cluster, since the Sn–Bi interchange rearrangement in $Sn_{10}Bi_2$ is rather similar (or of the same origin) with the Sn_{12}^{2-}–Sn_{12}^{1-} rearrangement.

Finally, a few additional examples have been presented illustrating extra directions for further functionalization. It is hoped that the present approach would be also useful for further rationalization and could stimulate future work, both experimental and theoretical, on these types of very interesting and very promising materials.

[1] S. M. Beck, J. Chem. Phys. **87**, 4233 (1987); Chem. Phys. **90**, 6306 (1989).
[2] H. Hiura, T. Miyazaki, and T. Kanayama, Phys. Rev. Lett. **86**, 1733 (2001).
[3] V. Kumar and Y. Kawazoe, Phys. Rev. Lett. **87**, 045503 (2001); Appl. Phys. Lett. **80**, 859 (2002).
[4] M. Mühlhäuser, G. E. Froudakis, A. D. Zdetsis, and S. D. Peyerimhoff, Chem. Phys. Lett. **204**, 617 (1993); G. E. Froudakis, A. D. Zdetsis, M. Mühlhäuser, B. Engels, and S. D. Peyerimhoff, J. Chem. Phys. **101**, 6790 (1994).
[5] N. Shao, S. Bulusu, and X. C. Zeng, J. Chem. Phys. **128**, 154326 (2008).
[6] E. N. Koukaras and A. D. Zdetsis, Organometallics **28**, 4308 (2009).
[7] L. R. Sita and R. D. Bickerstaff, J. Am. Chem. Soc. **111**, 6454 (1989).
[8] M. Brynda, R. Herber, P. B. Hitchcock, M. F. Lappert, I. Nowik, P. P. Power, A. V. Protchenko, A. Ruzicka, and J. Steiner, Angew. Chem. **118**, 4439 (2006).
[9] E. Rivard, J. Steiner, J. C. Fettinger, J. R. Giuliani, M. P. Augustine, and P. P. Power, Chem. Commun. (Cambridge) 4919 (2007).
[10] M.-H. Ge and J. D. Corbett, Inorg. Chem. **46**, 4138 (2007).
[11] R. Hoffmann, Angew. Chem., Int. Ed. Engl. **21**, 711 (1982).
[12] W. N. Lipscomb, Science **153**, 373 (1966).
[13] K. Wade J. Chem. Soc., Chem. Commun., **22** 989 (1971); M. A. Fox and K. Wade, Pure Appl. Chem. **75**, 1315 (2003).
[14] R. E. Williams, Chem. Rev. (Washington, D.C.) **92**, 177 (1992).
[15] D. M. P. Mingos Nature (London), Phys. Sci. **236**, 99 (1972); R. Mason, K. M. Thomas, and D. M. P. Mingos, J. Am. Chem. Soc. **95**, 3802 (1973).
[16] R. B. King, Chem. Rev. (Washington, D.C.) **101**, 1119 (2001); R. B. King, T. Heine, C. Corminboeuf, and P. R. Schleyer, J. Am. Chem. Soc. **126**, 430 (2004).
[17] P. R. Schleyer, C. Maerker, A. Dransfeld, H. Jiao, and N. J. R. E. Hommes, J. Am. Chem. Soc. **118**, 6317 (1996); Chem. Rev. (Washington, D.C.) **101**, 5 (2001), special issue on aromaticity, edited by P. R. Schleyer.
[18] A. D. Zdetsis, J. Chem. Phys. **127**, 014314 (2007); **127**, 244308 (2007).
[19] A. D. Zdetsis, J. Chem. Phys. **128**, 184305 (2008).
[20] A. D. Zdetsis, J. Phys. Chem. A **112**, 5712 (2008); Inorg. Chem. **47**, 8823 (2008); J. Chem. Phys. **130**, 064303 (2009).
[21] D. Y. Zubarev, A. N. Alexandrova, A. I. Boldyrev, L. F. Cui, X. Li, and L. S. Wang, J. Chem. Phys. **124**, 124305 (2006); D. Y. Zubarev, A. I. Boldyrev, L. F. Cui, X. Li, and L. S. Wang, J. Phys. Chem. A **109**, 11385 (2005).
[22] T. Slee, L. Zhenyang, and D. M. P. Mingos, Inorg. Chem. **28**, 2256 (1989); D. J. Wales, D. M. P. Mingos, T. Slee, and L. Zhenyang, Acc. Chem. Res. **23**, 17 (1990).
[23] D. J. Wales, Phys. Rev. A **49**, 2195 (1994).
[24] E. D. Jemmis, B. V. Prasad, S. Tsuzuki, and K. Tanabe, J. Phys. Chem. **94**, 5530 (1990).
[25] T. Gädt and L. Wesemann, Organometallics **26**, 2474 (2007).
[26] N. V. Sidgwick, *The Electronic Theory of Valence* (Clarendon, Oxford, 1927).
[27] E. Pyykko, Chem. Rev. (Washington, D.C.) **88**, 563 (1988).
[28] M. Kaupp and P. V. R. Schleyer, J. Am. Chem. Soc. **115**, 1061 (1993).
[29] G. Rodger, *Introduction to Coordination Solid State and Descriptive Organic Chemistry*, (McGraw-Hill, New York, 2000).
[30] A. D. Zdetsis, Phys. Rev. B **75**, 085409 (2007).
[31] R. W. Chapman, J. G. Kester, K. Folting, W. E. Streib, L. J. Todd, Inorg. Chem. **31**, 979 (1992).
[32] L. F. Cui, X. Huang, L. M. Wang, D. Y. Zubarev, A. I. Boldyrev, J. Li, and L. S. Wang, J. Am. Chem. Soc. **128**, 8390 (2006).
[33] L. F. Cui, L. M. Wang, and L. S. Wang, J. Chem. Phys. **126**, 064505 (2007).

[34] J. L. Little, M. A. Whitesell, J. G. Kester, K. Folting, and L. J. Todd, Inorg. Chem. **29**, 804 (1990).
[35] A. Trifonova, M. Wachtler, M. Winter, and J. O. Besenhard, Ionics **8**, 321 (2002).
[36] Z. P. Xia, Y. Lin, and Z. Q. Li, Mater. Charact. **59**, 1324 (2008).
[37] X. Li, H. Wang, A. Grubisic, D. Wang, K. H. Bowen, M. Jackson, and B. Kiran, J. Chem. Phys. **129**, 134309 (2008).
[38] A. D. Becke, J. Chem. Phys. **98**, 5648 (1993); C. Lee, W. Yang, and R. G. Parr, Phys. Rev. B **37**, 785 (1988); S. H. Vosko, L. Wilk, and M. Nusair, Can. J. Phys. **58**, 1200 (1980); P. J. Stephens, F. J. Devlin, C. F. Chabalowski, and M. J. Frisch, J. Phys. Chem. **98**, 11623 (1994).
[39] K. Eichkorn, F. Weigend, O. Treutler, and R. Ahlrichs, Theor. Chem. Acc. **97**, 119 (1997); A. Schäfer, C. Huber, and R. Ahlrichs, J. Chem. Phys. **100**, 5829 (1994).
[40] TURBOMOLE, Version 5.6, Universitat Karlsruhe, 2000.
[41] A. Bergner, M. Dolg, W. Küchle, H. Stoll, and H. Preuss, Mol. Phys. **80**, 1431 (1993); W. Kuechle, M. Dolg, H. Stoll, and H. Preuss, *ibid.* **74**, 1245 (1991); X. Cao and M. Dolg, J. Chem. Phys. **115**, 7348 (2001).
[42] D. Andrae, U. Haeussermann, M. Dolg, H. Stoll, and H. Preuss, Theor. Chim. Acta **77**, 123 (1990).
[43] F. Weigend and R. Ahlrichs, Phys. Chem. Chem. Phys. **7**, 3297 (2005).
[44] B. Metz, H. Stoll, and M. Dolg, J. Chem. Phys. **113**, 2563 (2000).
[45] M. J. Frisch, G. W. Trucks, H. B. Schlegel *et al.*, GAUSSIAN 03, Revision C.02 program package, Gaussian, Inc., Pittsburgh, PA, 2004.
[46] A. D. Zdetsis, Phys. Rev. A **64**, 023202 (2001); Rev. Adv. Mater. Sci. **11**, 56 (2006); Comput. Lett. **1**, 337 (2005); A. D. Zdetsis, in *Silicon Clusters*, special issue of J. Comput. Methods Sci. Eng. **7**, 257 (2007), edited by G. Maroulis and A. D. Zdetsis.
[47] P. Karamanis, D. Zhang-Negrerie, and C. Pouchan, Chem. Phys. **331**, 417 (2007).
[48] E. N. Esenturk, J. Fettinger, Y. F. Lam, and B. Eichhorn, Angew. Chem., Int. Ed. **43**, 2132 (2004).
[49] X. Yang, W. Jiang, C. B. Knobler, and M. F. Hawthorne, J. Am. Chem. Soc. **114**, 9719 (1992).